International Journal of Agriculture and Biosciences 2025 14(4): 664-673.
https://doi.org/10.47278/journal.ijab/2025.082

RESEARCH ARTICLE
eISSN: 2306-3599; pISSN: 2305-6622

Improving Agricultural Waste Reduction through Clay-Based Superhydrophobic Polymer Composites

Olga Rozhkova [1,2,*], Dana Ibraimova [3], Vitaly Rozhkov [2], Kuanyshbek Musabekov [3], Svetlana Maryinsky [4] and Valeriy Kulichikhin [5]

[1]Science and Technology Solutions, JSC, Almaty, Kazakhstan
[2]Saken Seifullin Kazakh Agrotechnical University, Astana, Kazakhstan
[3]Al Farabi Kazakh National University, Almaty, Kazakhstan
[4]Altai Geological and Ecological Institute LLP, Ust-Kamenogorsk, Kazakhstan
[5]A.V. Topchiev Institute of Petrochemical Synthesis, RAS, Moscow, Russia
*Corresponding author: olrozhkova@mymail.academy

ABSTRACT

The study aims to develop environmentally sustainable polymer composites using superhydrophobic clay (SHC) fillers derived from natural Kazakh deposits. These composites are designed to enhance the mechanical and thermal performance of agricultural packaging materials, thereby reducing polymer waste and extending product lifespan in agro-industrial applications. Two types of natural clays – montmorillonite from the Tagan deposit and halloysite from the Beloe Glinishche deposit – were modified using octadecylamine (ODA) and tetrakis(decyl)ammonium bromide (TKAB) to obtain SHC powders with contact angles exceeding 170º. These SHCs were incorporated into polypropylene (PP) and polyethylene (PE) matrices at varying concentrations (1–10%) using melt-mixing techniques. The resulting nanocomposites were analyzed through rheological, mechanical, and thermal testing, as well as X-ray diffraction (XRD), scanning electron microscopy (SEM), and infrared spectroscopy (IR). Both MMT SHC and HNT SHC showed excellent dispersion in nonpolar polymer matrices and significantly improved the composites' tensile strength, flexural modulus, and thermal stability – even at low filler concentrations (1–3%). Contact angles of 170° (MMT SHC) and 172° (HNT SHC) demonstrated highly stable lotus-effect properties. Sedimentation tests confirmed their high colloidal stability in nonpolar environments, while XRD and IR analyses verified successful intercalation of surfactants into the clay structure. The incorporation of superhydrophobic clay fillers into PE and PP matrices enhances composite durability and mechanical performance, offering a promising pathway toward reducing agricultural polymer waste. These findings support the use of local, eco-friendly clay resources to develop high-performance biocompatible composites for sustainable agricultural applications.

Keywords: Karaganda hallosyte clay; Organoclay; Polypropylene nanocomposites; Rheological properties; Tagan montmorillonite clay.

Article History
Article # 25-198
Received: 21-Apr-25
Revised: 09-May-25
Accepted: 14-May-25
Online First: 28-May-25

INTRODUCTION

In recent years, the development of polymer-clay nanocomposites has become a major focus in materials science due to the superior properties these materials offer over traditional composites. Incorporating clay particles into polymer matrices can significantly enhance the resulting materials' mechanical, thermal, and barrier properties even at low filler concentrations. These composites demonstrate improved stiffness, strength, and resistance to thermal degradation, making them ideal for a wide range of applications in industries, including automotive manufacturing, electronics, packaging, and construction.

Clays, particularly montmorillonite (MMT) and halloysite, possess layered structures that enable them to

Cite this Article as: Rozhkova O, Ibraimova D, Rozhkov V, Musabekov K, Maryinsky S and Kulichikhin V, 2025. Improving agricultural waste reduction through clay-based superhydrophobic polymer composites. International Journal of Agriculture and Biosciences 14(4): 664-673. https://doi.org/10.47278/journal.ijab/2025.082

A Publication of Unique Scientific Publishers

interact effectively with polymers, improving dispersion and interfacial bonding. Organophilic clays are ideal for producing polymer-clay composites due to their unique ability to penetrate nonpolar environments (Patel et al., 2006; Anthoulis et al., 2009; Mittal, 2009). This feature results from the modification of the surface of layered mineral particles by cationic surfactants. Many techniques have been developed to modify layered silicates, and their contact angles range from 100º or more (Pazos et al., 2015; Høgsaa et al., 2018; Liu et al., 2018; Cao et al., 2019; Karataş et al., 2022; Nuruzzaman et al., 2022; Wall et al., 2022; Liu et al., 2023).

The most effective clay minerals are those with higher contact angles (Luo et al., 2014; Gülen & Deler, 2024; Khan et al., 2024; Swain et al., 2024). Organophilic clays are referred to as superhydrophobic if their contact angle exceeds 150º (Patel et al., 2006; Anthoulis et al., 2009; Mittal, 2009; Chen et al., 2014; Choung et al., 2014; Luo et al., 2014; Pazos et al., 2015; Høgsaa et al., 2018; Liu et al., 2018; Cao et al., 2019; Karataş et al., 2022; Nuruzzaman et al., 2022; Wall et al., 2022; Liu et al., 2023). The higher the superhydrophobicity of the clay (near 180º), the more adapted it is to incorporate into a nonpolar polymer matrix. This kind of superhydrophobic clay (SHC) serves as filler material in the production of polymer composites (Anthoulis et al., 2009; Mittal, 2009; Chen et al., 2014; Choung et al., 2014; Luo et al., 2014; Pazos et al., 2015; Høgsaa et al., 2018; Liu et al., 2018; Cao et al., 2019; Karataş et al., 2022; Nuruzzaman et al., 2022; Wall et al., 2022; Liu et al., 2023; Sirisaksoontorn & Lerner, 2023). Today, the need for materials with improved mechanical, thermal, and technological properties cannot be overestimated (Chua & Lu, 2007; Li et al., 2010; Wang et al., 2010; Khan et al., 2024). Clay-polymer nanocomposites are a relatively new class of materials that demonstrate improved properties under very low stress levels compared to regular composite fillers (Khan et al., 2024; Swain et al., 2024).

The development of materials production in this area allows for the manufacture of lighter materials with a higher elastic modulus and a lower coefficient of linear thermal expansion. These characteristics make these materials desirable for several applications, including those requiring higher heat distortion temperatures, greater stiffness and robustness, and improved resistance properties (Gülen & Deler, 2024).

These materials are widely used in automotive, electronics, and construction industries due to their superior characteristics, which make them a suitable substitute for metal parts (Du et al., 2024; Prabhudeva & Karmakar, 2024; Swain et al., 2024).

Polypropylene (PP) is distinguished by its low cost, high heat distortion temperature, and exceptional versatility in properties and applications, making it a popular and convenient thermoplastic material (El Fadl et al., 2024; Feng et al., 2024). To improve the competitiveness of polymer solid materials in technical resin applications, it is important to increase their dimensional stability, heat distortion temperature, stiffness, robustness, barrier properties, and toughness without compromising on the ease of processing (Ahmadizadegan & Esmaielzadeh, 2023; Costanza-Sharifian & Najafi, 2023; Robinson et al., 2024). Nanocomposites are typically obtained with using SHC and PP or polyethylene (PE). To obtain a nanocomposite that satisfies all technical requirements, the properties of the SHC used need to be improved. Scientific papers typically touch on the use of organo-modified clays (Cloisite 20A, Cloisite 30B, Southern Clay Products, etc.) in the production of PP-clay composites when focusing on rheological properties. Our study focuses on Kazakhstan because the country has a vast supply of clay minerals, the best known being the Tagan deposit of MMT clays and the Karaganda deposit of halloysite clays. However, the potential of these deposits is understudied. MMT clay from the Tagan deposit is used to produce unique SHCs that have a contact angle of θ = 170º (Ibraimova et al., 2023; Rozhkova et al., 2023). The research aimed to develop a method for obtaining SHC with high contact angles (over 170º) from halloysite and halloysite clays and to assess the effect of these contact angles on the incorporation of the SHC into polymer matrices.

The scientific novelty consists in the fact that organoclays have higher contact angles closer to 180° (θ = 1700 for MMT SHC and θ = 171o for halloysite SHC). It is difficult to trap a water droplet on the flat surface of superhydrophobic powders even for a fraction of a second. They behave like mercury droplets, which appears to be owed to hydrogen bonds and the lotus effect. In previous studies, the highest contact angles obtained reached up to 157° (Chua & Lu, 2007; Li et al., 2010; Wang et al., 2010; Chen et al., 2014; Choung et al., 2014; Luo et al., 2014; Pazos et al., 2015; Høgsaa et al., 2018; Liu et al., 2018; Cao et al., 2019; Karataş et al., 2022; Nuruzzaman et al., 2022; Wall et al., 2022; Sirisaksoontorn & Lerner, 2023; Du et al., 2024; Feng et al., 2024; Gülen & Deler, 2024; Khan et al., 2024; Swain et al., 2024). The only way these droplets can be measured is through fast measurement techniques and numerous repetitions. The obtained superhydrophobic micro- and nanopowders demonstrate high stability in nonpolar environments.

MATERIALS & METHODS

Study Location

The study was conducted in 2023 at the Tagan (East Kazakhstan region, Kazakhstan) and Beloe Glinishche (Karaganda, Kazakhstan) fields. Add a map of the study area.

Materials

Clay Samples

MMT clay from the Tagan field is known for its high purity, containing approximately 95% MMT. Halloysite clay from the Beloe Glinishche field. The deposit contains about 82% halloysite, which naturally forms nanotubes (halloysite nanotubes, or HNTs). In addition, for the sake of comparison, the study included organophilic clay made from halloysite clays of the Karaganda deposit (halloysite deposit Beloe Glinishche), the contact angle of which equals θ=171o (HNT SHC).

Polymer Matrices

The materials used as polymer matrix were homopolymer PP samples produced by Sibur LLC, Russian Federation (melt flow index – 0.7g/10min, density – 940kg/m3) and homopolymer PE samples produced by Flagman TK LLP, Kazakhstan (melt flow index – 0.3g/10 min, density – 930kg/m3).

Obtaining SHC

To obtain the SHC, first, solutions of ODA and TKAB at a concentration of 1mol/L were prepared. Clay samples purified from impurities and washed using decantation method were placed into the same solutions, 100g each. The obtained suspension was then vigorously mixed for 12 hours at 70°C. After this modification, the suspension was washed a few times to remove excess cationic surfactant. The resulting samples were dried in a drying chamber until fully dry at 70°C. In the next step, these samples were pulverized and passed through a sieve with an opening of 63µm or less. Contact angles were measured using powdered SHC samples. Before measuring contact angles, the SHC powders were pressed by hand because of their stickiness. As a result, the procedure of measuring the contact angles of SHC samples caused no difficulties. A feature of these two types of SHCs is that MMT clay has a 1:2 type crystal structure, while HNT clay has a 1:2 type crystal structure. In addition, HNT clays are natural nanocomposites that take the form of a twisted tube, whereas MMT particles are usually micro-sized and come in the form of layered plates.

Preparation of PP-SHC Nanocomposite

Nanocomposite samples were prepared by mixing PP granules with SHC at a ratio of 99:1; 97:3; 95:5; 93:7, and 90:10, respectively. The nanocomposites were produced using SHC with contact angles equaling θ=170°C (from Tagan MMT) and θ=172°C (from Karaganda halloysite (Beloe Glinishche)). As a result, we obtained 20 nanocomposite samples. Laboratory composite batches were made using a PolyDrive twin-rotor mixer (Thermo Haake, Germany) equipped with a 100 cm3 electrically heated chamber with two unidirectionally rotating rotors.

Different types of PPs are distinguished by their molecular structure. Depending on the structure of PP isomers, their melting point can vary from 80 to 165-170°C, and their density ranges between 850 and 910kg/m^3. The reason for choosing PP over PE is that PP is less dense, harder, and more heat resistant than PE. PP is less susceptible to cracking when exposed to aggressive media compared to PE. To obtain a homogeneous mass, the process of mixing PP and PE with clays was repeated several times at different temperatures and points in time. Ultimately, PP and PE granules were mixed with SHC samples at 190 and 180°C, respectively, for 10 minutes with the extruder running at a speed above 60rpm. After mixing, the extrudate had a clear perfect molten structure with no lumps. The mixing was achieved through shearing in a narrow gap between the turns of complex configuration rotors and between rotors and the wall. A high shear rate was achieved by different rotor speeds. The obtained nanocomposite was used to form 8 cm long, 2 mm thick, and 4 mm wide plates to test their rheological properties on rheometers. The influence of clay concentration on the rheological properties of the copolymer melt was examined on a Rosand capillary rheometer (Malvern, Great Britain) and a RheoStress-600 rotary viscometer (Thermo Haake, Germany).

The capillary rheometer has two viscometric chambers with capillaries of a finite and conditionally "zero" length. The first one predominantly realizes shear flow, which allows plotting the flow curves of composite melts. The second one is responsible for converging flow, which mainly stretches the melt. The presence of two capillaries allows the true flow curves to be obtained using the method of two capillaries. The tests performed on the rotational rheometer involved two deformation regimes – shear flow at the shear rate in the range of 10–3-102c–1 and periodic harmonic oscillations in the field of linear mechanical behavior of the tested sample in the frequency range of 101-103c–1. In the course of the tests, the samples were deformed between a conical and a flat surface (the cone diameter was 20 mm, the angle between the cone's generatrices and the plane was 1 degree). Shear stresses and effective viscosity were found at a constant cone rotation speed. Both the elastic and viscous components of the elastic modulus were found at constant frequency and amplitude of its oscillations.

After the modification of clays with cationic surfactant molecules, the filler samples were washed several times to remove excess cationic surfactant. ODA and TKAB solutions were used as the hydrophobizers of clay particles.

Data Analysis

a) SHC from HNTs (HNT SHC) was obtained by modifying the particles of Beloe Glinishche halloysite with ODA. The contact angle was determined using pressed HNT SHC. Measurements were taken several times to ensure reliability. A droplet of distilled water was placed on top of the powder and the resulting HNT SHC contact angle averaged 172º.

b) Superhydrophobic MMT clay from the Tagan deposit (MMT SHC) was obtained by modifying the particles of Tagan MMT with TKAB. Once again, the contact angle was determined using pressed HNT SHC powder and was measured repeatedly to ensure the reliability of the results. The contact angle obtained by placing a droplet of distilled water on top of the MMT SHC powder averaged at 170º.

The data obtained through mechanical and rheological tests were analyzed using standard statistical methods

RESULTS & DISCUSSION

SHC Characteristics and Properties

Table 1 presents contact angle values and the images of water droplets on the surface of halloysite, MMT, HNT SHC, and MMT SHC powders.

Table 1: Contact angles of clays and their superhydrophobic types

Object	Images of water droplets on the surface of clay and SHC powders	Contact angle	Abbreviation
Halloysite, Beloe Glinishche field		19º	HNT
After hydrophobization with ODA (HNT SHC)		172º	HNT SHC
Tagan MMT		39º	MMT
After hydrophobization with TKAB		170º	MMT SHC

The reason behind the choice of the ODA modifier for HNT and TKAB for MMT was the fact that numerous studies have proven that the maximum contact angles for HNT are obtained by modifying it with ODA. The maximum contact angles of MMT are achieved with TKAB. The greater the contact angle, the better the intercalation of particles into the interpackage space of clay minerals. These SHC micro- and nanoparticles can demonstrate greater stability in nonpolar environments and penetrate solid polymer particles better. All of the tested SHC samples were treated with ultrasound before modification with the cationic surfactant using a colloid mill equipped with ultrasound. Fig. 1 demonstrates the kinetics of sedimentation determined optically.

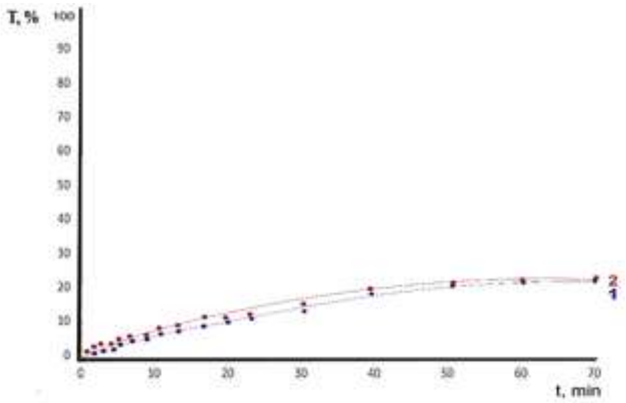

Fig. 1: Sedimentation kinetics of SHC samples in a hexane environment determined optically; 1 – MMT SHC; 2 – HNT SHC.

Fig. 1 shows that the maximum light transmittance of hexane in the presence of MMT SHC and HNT SHC particles is approximately 24%, which means that the solution remained cloudy even 70 minutes later. This suggests that SHC particles distribute best in nonpolar liquids (ε=2.1) and remain more stable in them. It can be concluded that the tested SHCs will easily distribute in a polymer matrix, as PP and PE are both nonpolar materials. It can be assumed that the intercalation of the cationic surfactant into the clay mineral proceeds according to Fig. 2.

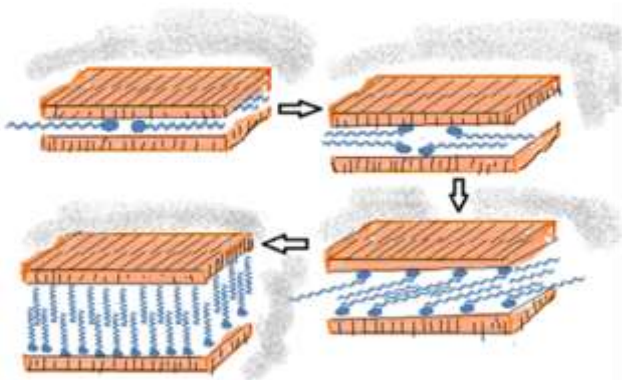

Fig. 2: Schematic illustration of the stage of intercalation of the cationic surfactant into the interpackage space of clay structure (Costanza-Robinson et al., 2024).

X-ray diffraction analysis successfully detects the introduction of any substances into the interpackage space and provides indisputable proof of the process of intercalation of the cationic surfactant into the interpackage space of clays. The results of X-ray diffraction analysis are presented in Fig. 3.

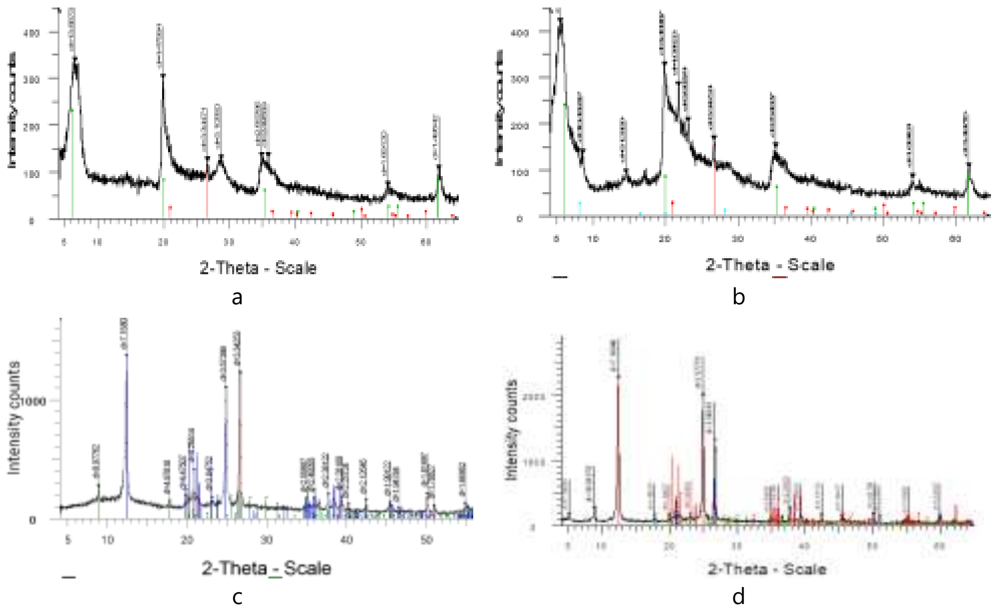

Fig. 3: X-ray diffraction analysis of clay and SHC samples; a – MMT; b – MMT SHC; c – HNT; d – HNT SHC.

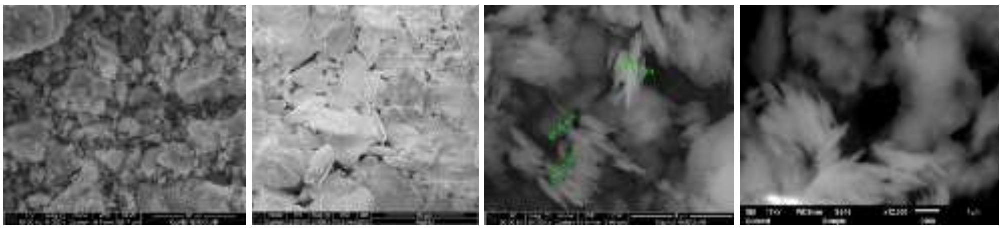

a b c d

Fig. 4: SEM images of MMT(a), MMT SHC(b), HNT(c), and HNT SHC (d).

As demonstrated in Fig. 1, after modification, the interpackage space changed from 13.84 to 16.61Å for MMT and from 9.9 to 17.50Å for HNT, indicating the intercalation process's success. Morphological changes after the modification of micro- and nanoparticles are also noticeable in the results of SEM analysis (Fig. 4).

The SEM images indicate morphological changes after the modification of micro- and nanoclays.

Infrared spectroscopy further proves the success of intercalation of surfactant molecules into the interpackage space by the presence of respective characterizing absorption bands for the cationic surfactant. Bands around 1,552 cm-1 corresponds to C-N bonds, peaks in the area of 1,471cm-1 describe the presence of oscillations corresponding to –CH2- bonds, and absorption bands around 2,861 and 2,936cm-1 correspond to C-H bonds in the hydrocarbon chain of the cationic surfactant.

Properties and Characteristics of PP and PE and their Composites with Clays

The viscosity of PP is of utmost importance in the molten state because it determines how easily a PP product can be extruded or injection molded. In fiber extrusion, melt elasticity is important to the processability of a PP product because it relates to how easily the material can be pulled into a fiber. Pseudoplastic fluids are characterized by a decrease in viscosity with increasing shear rate, which means that in pseudoplastic fluids the shear stress increases slower than the shear rate. Most polymer solutions and melts possess the properties of pseudoplastic liquids (Ahmadizadegan & Esmaielzadeh, 2023; Baruel et al., 2023; Cunha et al., 2023; Firmanda et al., 2023; Guo et al., 2023; Ibraimova et al., 2023; Peng et al., 2022; Rozhkova et al., 2023; Ulrich et al., 2023; Zeng et al., 2023; Liu et al., 2024; Sharifian & Najafi, 2023).

However, in the case of molded products from filled polymers, the filler introduced into the composition, being an active component of the system, can change the molecular and supramolecular structure of the polymer (the degree of its crystallinity, size, shape, the distribution of structural units for crystallizing polymers, etc.), which can lead to changes in the flow pattern of polymers.

The polymer crumbs used in our tests ranged in size from 2 to 3mm. To ensure an evenly mixed clay sample and PE, we tried to melt the mechanical mixture prepared in advance until the clay particles were evenly dispersed in the PP mixture.

Different types of PP are distinguished based on their molecular structure. Depending on the structure, the melting points of PP stereoisomers can vary from 80 to 165-170ºC and density ranges from 850 to 910kg/m^3. Our reason for choosing PP along with PE was that PP is less dense and harder and heat resistant compared to PE. Moreover, PP is less susceptible to cracking under the influence of aggressive media than PE.

In the course of the studies, we needed to obtain 20 samples of micro- and nanocomposites – five samples from the Tagan MMT (Fig. 5), five samples of SHC from the halloysite of the Beloe Glinishche deposit, and five samples of pure PP and PE each.

The composition and types of polymer-SHS composites are provided in Table 2. The rheological curves of PP and its nanocomposites are in Fig. 6 and 7.

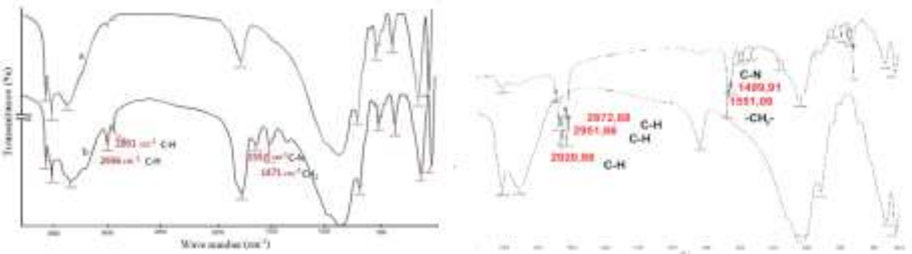

a b

Fig. 5: IR-spectra of clay samples; a – MMT and MMT SHC; b – HNT and HNT SHC.

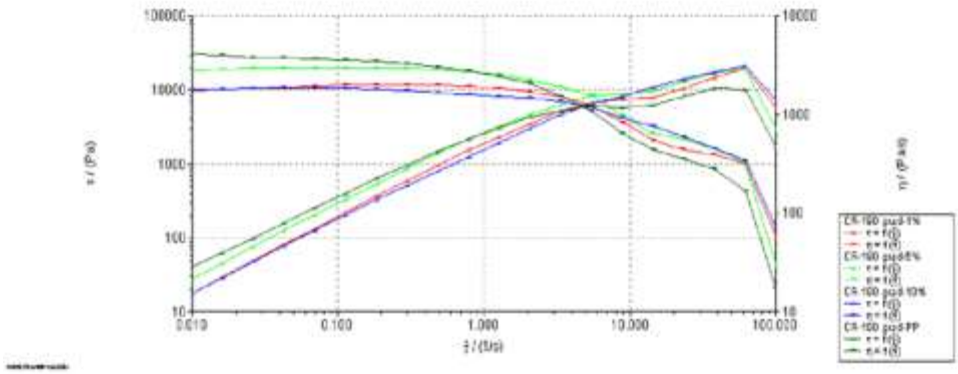

Fig. 6: Dependence of shear stress on shear rate in composites containing HNT SHC.

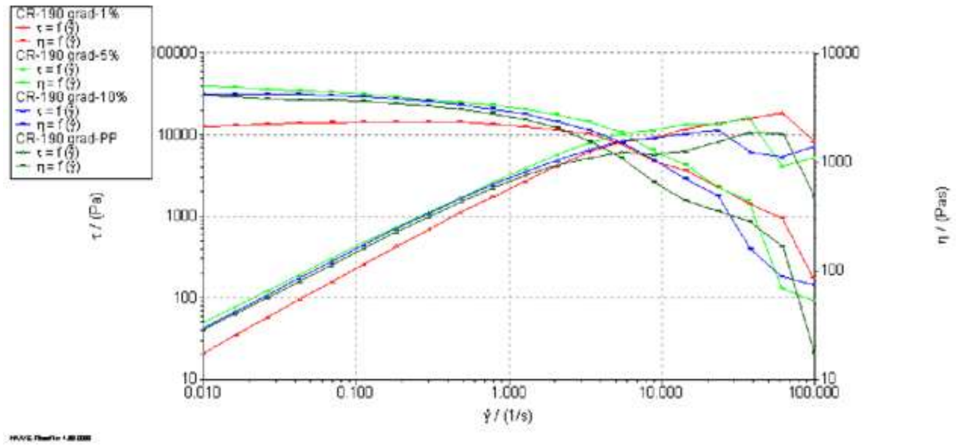

Fig. 7: Dependence of shear stress on shear rate in composites containing MMT SHC.

Table 2: Composition of the obtained micro- and nanocomposites containing SHC

No.	SHC content in the composite	Homopolymer matrix content in the composite, %	Abbreviation
1	1% MMT	99%PE	MMT-PE1
2	3% MMT	97% PE	MMT-PE3
3	5% MMT	95% PE	MMT-PE5
4	7% MMT	93% PE	MMT-PE7
5	10% MMT	90% PE	MMT-PE10
6	1% HNT	99% PE	HNT-PE1
7	3% HNT	97% PE	HNT-PE3
8	5% HNT	95% PE	HNT- PE5
9	7% HNT	93% PE	HNT-PE7
10	10% HNT	90% PE	HNT-PE10
11	1% MMT	99% PP	MMT-PP1
12	3% MMT	97% PP	MMT-PP3
13	5% MMT	95% PP	MMT-PP5
14	7% MMT	93% PP	MMT-PP7
15	10% MMT	90% PP	MMT-PP10
16	1% HNT	99% PP	HNT-PP1
17	3% HNT	97% PP	HNT-PP3
18	5% HNT	95% PP	HNT-PP5
19	7% HNT	93% PP	HNT-PP7
20	10% HNT	90% PP	HNT-PP10

Table 3 presents some physicomechanical characteristics of homopolymer PE and composite materials based on SHC samples and PE.

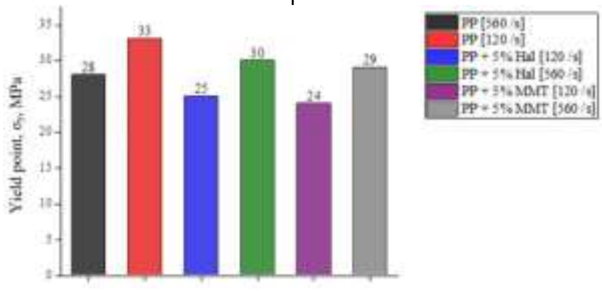

a

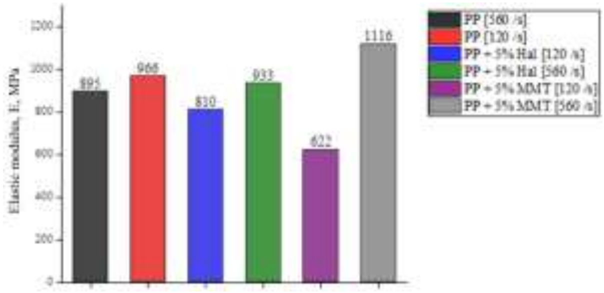

b

Fig. 8: Comparison of a) flow stress; b) yield point under uniaxial tension.

Table 3: Technical characteristics of the obtained PE composites with varying content of MMT or HNT

Composition of PP materials	Melt flow index, g/10min	Ultimate tensile strength at yield point, MPa	Elongation at yield point, %	Elongation at break, %	Flexural modulus, MPa	Crystallization start temperature, ºC
Homopolymeric PE	0.4	36.3	10	~200	1,620	130
MMT-PE1	4.72	44.5	10.65	~455	1,740	139
MMT-PE3	3.45	40.07	10.05	~100	1,667	132
MMT-PE5	3.69	42.5	10.35	~160	1,679	136
MMT-PE7	3.98	46.5	10.75	~425	1,720	154
MMT-PE10	3.82	49.8	10.85	~385	1,730	149
HNT-PE1	3.3	40.07	10.0	~210	1,765	133
HNT-PE3	3.39	42.3	10.1	~260	1,820	137
HNT-PE5	3.71	45.6	10.2	~320	1,850	139
HNT-PE7	3.79	47.3	10.5	~355	1,930	149
HNT-PE10	3.61	49.8	10.6	~198	1,940	145

Table 4: Technical characteristics of the obtained PP composites with varying content of MMT or HNT

Composition of PP materials	Melt flow index, g/10min	Ultimate tensile strength at yield point, MPa	Elongation at yield point, %	Elongation at break, %	Flexural modulus, MPa	Crystallization start temperature, ºC
Homopolymeric PP	0.8	36.3	10	~200	1,560	140
MMT-PP1	3.4	40.07	10.1	~200	1,565	141
MMT-PP3	3.69	41.32	10.4	~160	1,720	144
MMT-PP5	3.73	43.1	10.5	~220	1,750	147
MMT-PP7	3.78	46.8	10.7	~255	1,830	153
MMT-PP10	3.87	48.9	10.8	~295	1,840	157
HNT-PP1	4.3	49.8	10.47	~435	1,890	153
HNT-PP3	4.4	45.6	10.35	~310	1,780	147
HNT-PP5	4.1	40.07	10.0	~200	1,535	141
HNT-PP7	4.2	42.3	10.05	~280	1,710	144
HNT-PP10	4.3	47.3	10.55	~375	1,780	157

Table 4 and Fig. 8 show some physico-mechanical characteristics of homopolymer PP and composite materials based on SHC samples and PP.

As can be seen from Table 3, the addition of organoclays improves the physico-mechanical characteristics of composites based on PE and PP materials in all samples. It can be noted that the greatest improvement is demonstrated by the PE-organoclay composite containing 1% MMT SHC, whose ultimate tensile strength at yield point, flexural modulus, and elongation at yield point equal 44.5 MPa, 1,705 MPa, and 455%, respectively. Table 4 indicates that the most improved physico-mechanical properties are shown by the PE-organoclay composite with 1% HNT SHC, whose ultimate tensile strength at yield point, flexural modulus, and elongation at yield point are 49.8 MPa, 1890 MPa, and 435%, respectively.

A study by Sharifian and Najafi (2023) that focused on PP/organoclay/MAPP composites (MAPP being clay modifier) concluded that dispersion increases together with the MAPP/organoclay ratio, regardless of the total concentration of clay. The study found that high concentrations of MAPP improve clay dispersion and adhesion, thereby increasing the elastic modulus.

In our case, improved adhesion owes to the fact that ODA molecules, which possess a long hydrocarbon chain and sit on the surface of SHC particles, can improve the interaction between PP fibers and SHC particles. In the case of MMT SHC, the particles are predominantly micro-sized layered plates and therefore fit into the matrix of a homopolymer matrix much harder. Nevertheless, adhesion is achieved due to the presence of TKAB molecules on the surfaces and in the interpackage spaces of MMT particles.

Thus, our study thus shows that despite the microstructure of MMT, given high contact angle values, it is possible to obtain a composite material based on PE and MMT SHC. Furthermore, it is possible to produce a nanocomposite material based on PE with less MMT SHC filler (about 1%) if the contact angle is high enough (over 170º) and with smaller amounts of HNT SHC filler (around 1%) given a high contact angle (over 172º).

The incorporation of superhydrophobic clays (SHCs) into polypropylene (PP) and polyethylene (PE) matrices significantly enhanced the mechanical and thermal properties of the composites, supporting the growing body of evidence on the efficacy of nanoclay fillers in polymer reinforcement. The observed increase in tensile strength, flexural modulus, and thermal stability aligns with earlier studies demonstrating that modified nanoclays act as multifunctional fillers, reinforcing polymer matrices through strong filler-matrix interfacial interactions (Mostafaei & Zolriasatein, 2012). The successful intercalation of ODA into HNTs and TKAB into MMT, as confirmed by XRD and IR, reflects trends observed in similar clay-polymer systems. For instance, Jelić et al. (2021) reported that ODA-modified HNTs demonstrated expanded basal spacing and improved dispersion within nonpolar polymer matrices, resulting in enhanced mechanical properties of PP nanocomposites.

The current study's XRD results—showing an increase in interlayer spacing from 13.84 to 16.61 Å (MMT) and 9.9 to 17.50 Å (HNT)—are consistent with these findings and provide robust evidence of successful intercalation, which is critical for optimal filler performance. Moreover, the highly stable lotus-effect properties demonstrated by the SHC composites, with contact angles exceeding 170°, confirm the superhydrophobic nature of the fillers. Similar superhydrophobic PP composites were developed by Khattab et al. (2021), who also reported excellent dispersion and durability in nonpolar environments, reinforcing the sedimentation stability observed in our study. The rheological behavior of the composites indicated pseudoplastic flow characteristics, a well-documented phenomenon in polymer-clay systems (Arrigo & Malucelli, 2020). The addition of nanoclays often leads to a reduction in viscosity at higher shear rates, facilitating easier extrusion and molding. However, it is also known that nanofillers can alter the crystallinity and molecular arrangement of the polymer matrix. Prasad et al. (2020) demonstrated that nanoclay-filled PP composites exhibited modified crystallinity, leading to a balance between flow properties and mechanical strength, which correlates well with the present findings.

Morphological changes observed through SEM, such as the improved interfacial adhesion and dispersion of SHCs within the PP and PE matrices, are consistent with the microstructural analyses reported by Zhang et al. (2019), who highlighted the importance of clay dispersion in ensuring optimal mechanical performance of polymer-clay composites. Thermal stability, a critical parameter for agricultural applications, was also significantly improved in the current study. Peng et al. (2018) demonstrated that nanoclay-modified PP composites exhibited higher decomposition temperatures and reduced thermal degradation rates, which were attributed to the barrier effect of the clay layers. These findings directly support the observed thermal improvements in our composites.

The choice of local Kazakh clays (Tagan MMT and Beloe Glinishche HNT) not only underscores the importance of utilizing indigenous resources but also resonates with sustainable material development goals. A recent study by Ihekweme et al. (2020) highlighted the potential of Central Asian clay minerals for advanced material applications, affirming the significance of this approach. In conclusion, the integration of SHC fillers into PP and PE matrices successfully enhanced the composites' mechanical strength, thermal stability, and superhydrophobicity, offering a promising avenue for reducing agricultural plastic waste. This study aligns with recent advances in polymer-clay nanocomposites and highlights the untapped potential of local clay resources for developing sustainable agro-industrial materials.

Conclusions

Our studies are first to obtain superhydrophobic micro- and nanopowders with contact angles approaching 180º.

Specifically, we reported the first instance of obtaining HNT SHC with a contact angle of 172º by modifying HNT from the Beloe Glinishche deposit with ODA. In addition, MMT SHC with a contact angle of 170º was produced through the modification of the microparticles of MMT from the Tagan deposit.

The experiments showed that on the surface of micro- and nanopowders of SHCs, water droplets behave like mercury droplets, which vividly demonstrates the lotus effect.

It was experimentally proven that the studied superhydrophobic micro- and nanopowders demonstrate high stability (do not settle for 70min and show a turbidity of 75% without changes) in a hexane environment (as an example of a nonpolar environment).

The new micro- and nano powders were used to obtain composite materials based on PP and PE. The experiments showed that the consumption of organoclay to produce the composite decreases with the introduction of SHCs with higher contact angles in contrast to similar SHCs with lower contact angles, which is an economically advantageous aspect for their further production.

DECLARATIONS

Funding: This scientific research was funded by a from the Kazakhstan state government scientific projects AP19674742 (IRN) "Technology for obtaining a new organo-mineral composite material based on natural bentonite of East Kazakhstan". The funding source was the Science Committee of the Ministry of Science and Higher Education of the Republic of Kazakhstan. The authors express their gratitude for this allocated grant funding.

Acknowledgement: The authors gratefully acknowledge the editorial team of the International Journal of Agriculture and Biology for their valuable feedback, guidance, and support throughout the review and publication process.

Conflicts of Interest: The authors declare no conflict of interest.

Data Availability: All the data is inside the article.

Ethics Statement: This research did not involve human participants or animals and therefore did not require ethical approval. All experiments and procedures were conducted in accordance with institutional guidelines and applicable national research standards.

Author's Contributions: Olga Rozhkova: Project administration, conceptual design, methodology, writing – original draft; Dana Ibraimova: Synthesis of superhydrophobic clay fillers, contact angle measurements, IR and XRD analysis; Vitaly Rozhkov: Rheological and thermal analysis, data interpretation; Kuanyshbek Musabekov: Preparation of polymer-clay nanocomposites, SEM analysis; Svetlana Maryinsky: Resource analysis of clay deposits, contribution to materials section; Valeriy Kulichikhin: validation of rheological methods, manuscript editing.

Generative AI Statement: The authors declare that no Gen AI/DeepSeek was used in the writing/creation of this manuscript.

Publisher's Note: All claims stated in this article are exclusively those of the authors and do not necessarily represent those of their affiliated organizations or those of the publisher, the editors, and the reviewers. Any product that may be evaluated/assessed in this article or claimed by its manufacturer is not guaranteed or endorsed by the publisher/editors.

REFERENCES

Ahmadizadegan, H., & Esmaielzadeh, S. (2023). Synthesis and characterization of new nanocomposites-based polyimide/modified montmorillonite and their applications in gas separation. *Polymer-Plastics Technology and Materials*, 62(10), 1329–1346. https://doi.org/10.1080/25740881.2023.2207101

Anthoulis, G.I., Kontou, E., Fainleib, A., & Bei, I. (2009). Polytetramethylene glycol-modified polycyanurate matrices reinforced with nanoclays: Synthesis and thermomechanical performance. *Mechanics of Composite Materials*, 45(2), 175–182. https://doi.org/10.1007/s11029-009-9073-x

Arrigo, R., & Malucelli, G. (2020). Rheological behavior of polymer/carbon nanotube composites: An overview. *Materials*, 13(12), 2771. https://doi.org/10.3390/ma13122771

Baruel, A.F., Dutra, R.C.L., Diniz, M.F., Azevedo, M.F.P., & Cassu, S.N. (2023). The role of organoclay in the diffusion of epoxy-amine oligomers and in the cross-linking density of the resulting network. *Journal of Applied Polymer Science, 140*(9), e53571. https://doi.org/10.1002/app.53571

Cao, G., Gao, M., Shen, T., Zhao, B., & Zeng, H. (2019). Comparison between Asymmetric and Symmetric Gemini Surfactant-Modified Novel Organo-vermiculites for Removal of Phenols. *Industrial and Engineering Chemistry Research*, 58(29), 12927–12938. https://doi.org/10.1021/acs.iecr.9b02997

Chen, S., Zhou, W., Cao, Y., Xue, C., & Lu, C. (2014). Organo-modified montmorillonite enhanced chemiluminescence via inactivation of halide counterions in a micellar solution. *The Journal of Physical Chemistry C, 118*(5), 2851–2856. https://doi.org/10.1021/jp411290z

Choung, S., Kim, M., Yang, J.S., Kim, M.G., & Um, W. (2014). Effects of radiation and temperature on iodide sorption by surfactant-modified bentonite. *Environmental Science and Technology*, 48(16), 9684–9691. https://doi.org/10.1021/es501661z

Chua, Y.C., & Lu, X. (2007). Polymorphism behavior of poly (ethylene naphthalate)/clay nanocomposites: Role of clay surface modification. *Langmuir, 23*(4), 1701-1710. https://doi.org/10.1021/la0626048

Costanza-Robinson, M.S., Payne, E.M., Dellinger, E., Fink, K., Bunt, R.C., Littlefield, M., Mejaes, B.A., Morris, R.K., Pincus, L.N., & Wilcox, E.H. (2024). Influence of water saturation on interlayer properties of HDTMA-, HDTMP-, and HDPy-modified montmorillonite organoclays. *Applied Clay Science*, *247*. https://doi.org/10.1016/j.clay.2023.107188

Cunha, R.V., Morais, A.I.S., Trigueiro, P., de Souza, J.S.N., Damacena, D.H.L., Brandão-Lima, L.C., Bezerra, R.D.S., Fonseca, M.G., Silva-Filho, E.C., & Osajima, J.A. (2023). Organic–Inorganic Hybrid Pigments Based on Bentonite: Strategies to Stabilize the Quinoidal Base Form of Anthocyanin. *International Journal of Molecular Sciences*, *24*(3). https://doi.org/10.3390/ijms24032417

Du, Q., Chen, S., Liu, H., Zhang, M., Ren, S., & Luo, W. (2024). Sequential modification of montmorillonite by Al13 polycation and cationic gemini surfactant for the removal of Orange II. *Colloids and Surfaces A: Physicochemical and Engineering Aspects*, *687*. https://doi.org/10.1016/j.colsurfa.2024.133489

El Fadl, F.I.A., El-Toony, M.M., & Maziad, N.A. (2024). Application of Tea Waste/Alginate/Nanoparticles Iron Bio-nanocomposite Beads for Removal of Crude Oil. *Journal of Polymers and the Environment*, *32*(2), 780–790. https://doi.org/10.1007/s10924-023-02969-w

Feng, J., Guo, J., Tang, R., Li, J., Su, X., & Hua, R. (2024). The effect of surfactants on the efficiency and consumption of acid stirred leaching of uranium ore. *Journal of Radioanalytical and Nuclear Chemistry*, *333*(4), 1873–1881. https://doi.org/10.1007/s10967-024-09405-w

Firmanda, A., Fahma, F., Syamsu, K., Sari, Y.W., Suryanegara, L., Wood, K., & Saito, Y. (2023). Factors influencing the biodegradability of agro-biopolymer based slow or controlled release fertilizer. *Journal of Polymers and the Environmen, 31*(5), 1706-1724. https://doi.org/10.1007/s10924-022-02718-5

Gülen, J., & Deler, Ö. (2024). The potential capability of treated perlite for removal of penta chloro nitrobenzene. *Zeitschrift Fur Physikalische Chemie*, *238*(6), 1103–1121. https://doi.org/10.1515/zpch-2023-0321

Guo, D., Wan, Y., Li, J., Liu, R., Liu, L., & Xue, Q. (2023). Comparative assessment of modified bentonites as retardation barrier: adsorption performance and characterization. *Environmental Earth Sciences*, *82*(2). https://doi.org/10.1007/s12665-022-10690-5

Høgsaa, B., Fini, E. H., de Claville Christiansen, J., Hung, A., Mousavi, M., Jensen, E.A., Pahlavan, F., Pedersen, T.H., & Sanporean, C.-G. (2018). A Novel Bioresidue to Compatibilize Sodium Montmorillonite and Linear Low Density Polyethylene. *Industrial and Engineering Chemistry Research*, *57*(4), 1213–1224. https://doi.org/10.1021/acs.iecr.7b04178

Ibraimova, D.M-K., Rozhkova, O.V., Musabekov, K.B., Tazhibayeva, S.M., Rozhkov, V.I., & Yermekov, M.T. (2023). Development of Methods to Obtain Composite Materials from Organoclays. *Eurasian Journal of Chemistry*, *112*(4), 101–111. https://doi.org/10.31489/2959-0663/4-23-14

Ihekweme, G.O., Shondo, J., Orisekeh, K.I., Kalu-Uka, G.M., Nwuzor, I.C., & Onwualu, A.P. (2020). Characterization of certain Nigerian clay minerals for water purification and other industrial applications. *Heliyon*, *6*(4), e03783–e03783. https://doi.org/10.1016/j.heliyon.2020.e03783

Jelić, A., Marinković, A., Sekulić, M., Dikić, S., Ugrinović, V., Pavlović, V.B., & Putić, S. (2021). Design of halloysite modification for improvement of mechanical properties of the epoxy based nanocomposites. *Polymer Composites*, *42*(5), 2180–2192. https://doi.org/10.1002/pc.25967

Karataş, D., Bahadori, F., Tekin, A., Kizilcay, G.E., & Celik, M.S. (2022). Enhancing the Kinetic Stability of Polymeric Nanomicelles (PLGA) Using Nano-Montmorillonite for Effective Targeting of Cancer Tumors. *Journal of Physical Chemistry B*, *126*(2), 463–479. https://doi.org/10.1021/acs.jpcb.1c07334

Khan, M.I., Howladar, M.F., Das, P., Hossain, M.N., & Yasin, M. (2024). Application of black tea waste as eco-friendly deflocculant and rheology stabilizer for water-based mud. *Geoenergy Science and Engineering*, *239*, 212956. https://doi.org/10.1016/j.geoen.2024.212956

Khattab, T.A., Tolba, E., Gaffer, H.E., & Kamel, S. (2021). Development of Electrospun Nanofibrous-Walled Tubes for Potential Production of Photoluminescent Endoscopes. *Industrial & Engineering Chemistry Research*, *60*(28), 10044–10055. https://doi.org/10.1021/acs.iecr.1c01519

Li, Z., Jiang, W.-T., Chen, C.-J., & Hong, H. (2010). Influence of chain lengths and loading levels on interlayer configurations of intercalated alkylammonium and their transitions in rectorite. *Langmuir, 26*(11), 8289-8294. https://doi.org/10.1021/la904677s

Liu, M.-L., Huang, M., Tian, L.-Y., Zhao, L.-H., Ding, B., Kong, D.-B., Yang, Q.-H., & Shao, J.-J. (2018). Two-Dimensional Nanochannel Arrays Based on Flexible Montmorillonite Membranes. *ACS Applied Materials and Interfaces*, *10*(51), 44915–44923. https://doi.org/10.1021/acsami.8b17719

Liu, Y., Xia, Z., Wang, Y., Rozyyev, V., Kazi, O.A., Gao, F., Wang, D., Lee, S.S., Koritala, R., Wen, J., Elam, J. W., & Darling, S.B. (2023). Montmorillonite Membranes with Tunable Ion Transport by Controlling Interlayer Spacing. *ACS Applied Materials and Interfaces*. https://doi.org/10.1021/acsami.3c13678

Liu, Y., Cao, G., Cheng, Q., Bai, Y., Zhang, N., & Zhai, S. (2024). Montmorillonite swelling properties with various surfactants based on molecular simulation. *Journal of Dispersion Science and Technology*, *45*(8), 1613–1622. https://doi.org/10.1080/01932691.2023.2225587

Luo, Z., Gao, M., Gu, Z., & Ye, Y. (2014). Structures and wettability alterations of a series of bispyridinium dibromides exchanged with reduced-charge montmorillonites. *Energy Fuels, 28*(9), 6163-6171. https://doi.org/10.1021/ef5011385

Mittal, V. (2009). Polymer layered silicate nanocomposites: A review. *Materials, 2*(3), 992-1057. https://doi.org/10.3390/ma2030992

Mostafaei, A., & Zolriasatein, A. (2012). Synthesis and characterization of conducting polyaniline nanocomposites containing ZnO nanorods. *Progress in Natural Science Materials International*, *22*(4), 273–280. https://doi.org/10.1016/j.pnsc.2012.07.002

Nuruzzaman, M., Liu, Y., Ren, J., Rahman, M.M., Zhang, H., Johir, M.A.H., Shon, H.K., & Naidu, R. (2022). Capability of Organically Modified Montmorillonite Nanoclay as a Carrier for Imidacloprid Delivery. *ACS Agricultural Science and Technology*, *2*(1), 57–68. https://doi.org/10.1021/acsagscitech.1c00125

Patel, H.A., Somani, R.S., Bajaj, H.C., & Jasra, R.V. (2006). Nanoclays for polymer nanocomposites, paints, inks, greases and cosmetics formulations, drug delivery vehicle and waste water treatment. *Bulletin of Materials Science*, *29*(2), 133–145. https://doi.org/10.1007/BF02704606

Pazos, M.C., Cota, A., Osuna, F.J., Pavón, E., & Alba, M.D. (2015). Self-assembling of tetradecylammonium chain on swelling high charge micas (Na-Mica-3 and Na-Mica-2): Effect of alkylammonium concentration and mica layer charge. *Langmuir, 31*(15), 4394-4401. https://doi.org/10.1021/acs.langmuir.5b00224

Peng, W., Cui, Z., Fu, H., Cao, H., Chen, M., Zhang, D., Luo, W., & Ren, S. (2022). Grafting of R4N+-Bearing Organosilane on Kaolinite, Montmorillonite, and Zeolite for Simultaneous Adsorption of

Ammonium and Nitrate. *International Journal of Environmental Research and Public Health*, *19*(19). https://doi.org/10.3390/ijerph191912562

Peng, Y., Nair, S.S., Chen, H., Yan, N., & Cao, J. (2018). Effects of Lignin Content on Mechanical and Thermal Properties of Polypropylene Composites Reinforced with Micro Particles of Spray Dried Cellulose Nanofibrils. *ACS Sustainable Chemistry & Engineering*, *6*(8), 11078–11086. https://doi.org/10.1021/acssuschemeng.8b02544

Prabhudeva, P., & Karmakar, S. (2024). Investigation on stability and energy potential of boron-loaded slurry fuel with higher loadings. *Advanced Powder Technology*, *35*(3). https://doi.org/10.1016/j.apt.2024.104363

Prasad, K.H., Ravichandran, K., Jayaseelan, V., & Muthuramalingam, T. (2020). Acoustic and mechanical characterisation of polypropylene composites reinforced by natural fibres for automotive applications. *Journal of Materials Research and Technology*, *9*(6), 14029–14035. https://doi.org/10.1016/j.jmrt.2020.09.112

Rozhkova, O.V., Muzdybayeva, S.A., Musabekov, K.B., Ibraimova, D.M.-K., Rozhkov, V.I., & Yermekov, M.T. (2023). Development of methods for obtaining drug carriers based on organomodified clays. *News of the National Academy of Sciences of the Republic of Kazakhstan. Series of Chemistry and Technology Sciences, 3*, 138-156.

Sharifian, S., & Najafi, H. (2023). Adsorption process of antibiotics by clay-based materials. In Traditional and Novel Adsorbents for Antibiotics Removal from Wastewater (pp. 217–299). Elsevier. https://doi.org/10.1016/B978-0-443-19211-1.00003-4

Sirisaksoontorn, W., & Lerner, M.M. (2023). Preparation of a homologous series of tetraalkylammonium graphite intercalation compounds. *Inorganic Chemistry*, *52*(12), 7139–7144. https://doi.org/10.1021/ic400733k

Swain, R., Nandi, S., Mohapatra, S., & Mallick, S. (2024). Engineered Clay-Polymer Composite for Biomedical Drug Delivery and Future Challenges: A Survey. *Current Drug Delivery*, *21*(5), 645–661. https://doi.org/10.2174/1567201820666230410110206

Ulrich, G.D., Lemos, A.G., Silva-Alvarez, A.C.F., Paiva, L.B., Gavioli, R.R., da Silva, L.L., de Freitas, O., & Francisco, K.R. (2023). Zein/hydroxypropylcellulose biofilms with hydrophilic and hydrophobic montmorillonite clays. *Polymer Composites*, 44(5), 2634–2644. https://doi.org/10.1002/pc.27266

Wall, N.A., Maulden, E., Gager, E.J., Ta, A.T., Ullberg, R.S., Zeng, G. Nava-Farias, L., Sims, A.P., Nino, J.C., Phillpot, S.R., Szecsody, J.E., & Pearce, C.I. (2022). Functionalized clays for radionuclide sequestration: A review. *ACS Earth and Space Chemistry, 6*(11), 2552-2574. https://doi.org/10.1021/acsearthspacechem.2c00098

Wang, T.-H., Hsieh, C.-J., Lin, S.-M., Wu, D.-C., Li, M.-H., & Teng, S.-P. (2010). Effect of alkyl properties and head groups of cationic surfactants on retention of cesium by organoclays. *Environmental Science and Technology*, 44(13), 5142–5147. https://doi.org/10.1021/es100349k

Zeng, W., Huang, W., Guo, B., Sun, Y., & Shen, H. (2023). Preparation and lubricating properties of polystyrene composite microspheres. *Materials, 16*(8), 3071. https://doi.org/10.3390/ma16083071

Zhang, F., Wang, J., Liu, T., & Shang, C. (2019). Enhanced mechanical properties of few-layer graphene reinforced titanium alloy matrix nanocomposites with a network architecture. *Materials & Design*, *186*, 108330. https://doi.org/10.1016/j.matdes.2019.108330